Open access • Journal Article • DOI:10.1007/S11721-017-0137-6

The impact of agent density on scalability in collective systems: noise-induced versus majority-based bistability — Source link

Yara Khaluf, Carlo Pinciroli, Gabriele Valentini, Heiko Hamann

Institutions: Ghent University, Worcester Polytechnic Institute, Arizona State University, University of Lübeck

Published on: 17 May 2017 - Swarm Intelligence (Springer US)

Topics: Swarm behaviour, Majority rule and Scalability

Noname manuscript No.
(will be inserted by the editor)

The Impact of Agent Density on Scalability in Collective Systems: Noise-Induced vs Majority-Based Bistability

Yara Khaluf · Carlo Pinciroli · Gabriele Valentini · Heiko Hamann

the date of receipt and acceptance should be inserted later

Y. Khaluf
Department of Information Technology
Ghent University
Ghent, Belgium
E-mail: yara.khaluf@ugent.be

C. Pinciroli
Robotics Engineering and Computer Science
Worcester Polytechnic Institute
Worcester, USA
E-mail: cpinciroli@wpi.edu

G. Valentini
School of Earth and Space Exploration
Arizona State University
Arizona, USA
E-mail: gvalentini@asu.edu

H. Hamann
Institute of Computer Engineering
University of Lübeck
Lübeck, Germany
E-mail: hamann@iti.uni-luebeck.de

Abstract In this paper, we show that non-uniform distributions in swarms of agents have an impact on the scalability of collective decision-making. In particular, we highlight the relevance of noise-induced bistability in very sparse swarm systems and the failure of these systems to scale. Our work is based on three decision models. In the first model, each agent can change its decision after being recruited by a nearby agent. The second model captures the dynamics of dense swarms controlled by the majority rule (i.e., agents switch their opinion to comply with that of the majority of their neighbors). The third model combines the first two, with the aim of studying the role of non-uniform swarm density in the performance of collective decision-making. Based on the three models, we formulate a set of requirements for convergence and scalability in collective decision-making.

Keywords bistable system, swarm density, noise, collective decision-making, nonuniform spatial distribution

1 Introduction

One of the key advantages of swarm intelligence is scalability. A swarm system is scalable because it "can maintain its function while increasing its size without the need to redefine the way its parts interact" [5]. The selection of the modeling technique used to analyze scalability properties covers a pivotal role. Assuming the limit $N \to \infty$ for the swarm size N allows for the definition of concise mathematical models, such as population models (e.g., rate equations [26, 24], birth-death processes [22]). However, the predictions of these models can differ qualitatively from the dynamics of actual finite-size systems [40, 29, 4]. For example, a finite-size system can show variance due to errors that result from the drawing of a finite number of samples from a stochastic population. Such effects are difficult to represent in a population model [42]. When investigating properties of scalability in collective systems, however, we have to consider finite-size effects as well as effects of noise, which can be similar to those caused by sampling errors. For example, agents may have communication errors due to a noisy communication medium. As a consequence agents may act sometimes erroneously. The effect of that behavior is similar to finite-size effects and increases the variance in the observed system states.

In this paper, we focus on the scalability of self-organizing collective decision-making systems, a fundamental process in autonomous swarm systems. We study which features influence the scalability of this process, including the effects of swarm density, noise, and non-uniform spatial distributions of agents. First, we show how a simple model of noise-induced bistability [29] is unable to scale in a very sparse distribution of agents. Next, we show a modification of this model that manages to reach a collective decision through the majority rule. This model effectively corresponds to a dense distribution of agents. Finally, we combine the two models to investigate a continuum of swarm densities and formulate the requirements to ensure scalability in collective systems. The paper is organized as follows. In Section 2, we discuss related work. Section 3 introduces a set of fundamental definitions. In Section 4, we present the models that we study and that represent different swarm densities: very sparse, sparse, dense. Our results are presented in Section 5. In Section 6 we introduce density defined independent of noise and we show the dynamics of the system while moving from an undecided system to a decided one. We verify our findings using agent-based simulations in Section 7 and the paper is concluded in Section 8.

2 Related work

A number of scientific studies report on decision-making in ants [3, 25], honeybees [36, 39], cockroaches [12], locusts [45], social spiders [34], and robots [11, 28, 41, 42, 44]. In the following we focus on binary decision-making problems that can be viewed as bistable systems. Bistable systems spend most of their time in one of two stable states while transitions between stable states occur rarely in response to external input, such as external noise.

Traditionally, bistable systems were modeled deterministically [9]. However, a recently discovered mechanism for bistability in the context of chemical systems has triggered a new track of research. There are chemical systems that behave qualitatively differently if there are only few molecules (i.e., low concentration or low density) [40, 29]. In these systems, the very existence of bistable states is induced by noise and consequently they cannot be modeled with standard techniques. Recently, Biancalani et al. [4] have made an effort to transfer the knowledge about

noise-induced bistable systems from the domain of chemistry to the domain of swarm intelligence. They investigate foraging in ants as a bistable system with an abstract model (also cf. [16]) that was reported before in the context of chemical reactions by Ohkubo et al. [29]. We use the model of Biancalani et al. [4] as a starting point to investigate scalability issues in collective systems with respect to swarm size, swarm density, noise, and finite size effects.

Bistable systems and the relevance of noise as well as of negative feedback processes have already been investigated in the context of swarm intelligence. Similar to our approach, Dyson et al. [7] propose a minimal model for the collective motion of locust swarms based on the model given by Biancalani et al. [4]. Dyson et al. consider different swarm densities by deriving drift and diffusion coefficients of a stochastic differential equation as a function of the swarm sizes. This is done by starting from experimental data and fitting the reaction rate coefficients that correspond to interactions between two or three agents (we refer to as second- and third-order interactions). In contrast to our study, they are investigating combinations of second- and third-order interactions for a few given measurements in a phenomenological way, while we investigate the continuum of swarm densities between second- and third-order interactions in the context of node degree variance in a network of agents.

Meyer et al. [27] highlight the influence of noise for achieving adaptivity in the foraging behavior of ants. They also show that certain system features are not captured well with the available mathematical models. Their investigation of the y-shaped bridge experiment as a binary decision-making problem shows that convergence to the shortest path as predicted by the applied mathematical models only holds if both choices have been presented to the colony at the same time. However, if the inferior choice is presented first, the colony sticks to that solution and does not adapt to the better path. This problem is solved by noise in the swarm's decision-making behavior: noise increases the explorative behavior of the system which is a necessary condition to achieve adaptiveness. Dussutour et al. [6] show the importance of noise in the behavior of ants that efficiently choose food sources in dynamic environments. They argue that a certain level of noise serves an important functional role in self-organized decision-making. Gruter et al. [10] investigate the role of negative feedback due to crowding in a foraging

scenario both experimentally and with an agent-based simulation model. They show that negative feedback leads to an equal distribution of foragers in symmetric environments and allows the majority of the colony to quickly reallocate to the best source in dynamic environments. Seeley et al. [37] focus on the influence of stop signals in collective decision-making processes. They provide an analytic model that shows the effect of cross-inhibition. The negative feedback by stop signals increases the reliability of the decision-making process because it solves the problem of deadlocks and triggers bistable distributions (cf. [31, 32]). In [23] the authors investigated the role of positive/negative feedbacks in addition to noise in the emergence of self organization and collective decision-making.

3 Preliminaries

In this section, we specify terms, such as swarm density, agent interactions, well-mixed systems, and noise. We introduce appropriate definitions to clarify our models and assumptions.

3.1 Swarms modeled as undirected graphs

A given spatial distribution of agents induces a graph based on neighborhood relations between pairs of agents. Two agents are neighbors if they perceive each other. Even though the range of existing sensors, such as infrared, radio, or sound sensors, depends on multiple features and is complex to model, in this paper, we use the simple unit disc model, which suffices for our purposes. We assume that sensing is pairwise symmetric, that is, if agent i senses agent j, then agent j also senses agent i. Agents perceive each other and establish a communication link once their distance is below a defined sensor range u. Based on these pairwise relations, we can construct an undirected graph with a node for each agent and an edge for each pair of neighboring agents. The neighborhood size and the node degree of a particular agent are the number of agents within its communication range u excluding the agent itself. The group size also includes the considered agent and is defined as the neighborhood size plus one.

3.2 Swarm density

We define three density classes for swarms. Our definition of density is based exclusively on node degrees, that is, the number of neighbors an agent can interact with[1]. The node degrees are determined by the spatial distribution of agents. In swarm robotics, the spatial distribution is generally a non-trivial result of the swarm behavior. We consider a static network model as an example here—the well-known Poisson Point Process (PPP) for which Poisson-distributed node degrees are generated [38]. The probability of finding a node of degree k is given by

$$P(X = k) = e^{-\lambda} \frac{\lambda^k}{k!}, \tag{1}$$

where λ is defined as the expected node degree. The Poisson distribution describes directly the above mentioned variance in the node degree due to the uniform random distribution of points. Here, we focus on particular swarm densities that create three different node distributions depending on whether most nodes have a node degree of one or less, two or less, or two and more. We define the probabilities

$$P_{k\leqslant 1} = P(X = 0) + P(X = 1), \tag{2}$$

$$P_{k\leqslant 2} = \sum_{k\leqslant 2} P(X = k), \tag{3}$$

$$P_{k\geqslant 2} = \sum_{k\geqslant 2} P(X = k). \tag{4}$$

If $P_{k\leqslant 1} > 0.5$, we consider the system as a very sparse system, if $P_{k\leqslant 2} > 0.5$, we consider the system as a sparse system, and for values of $P_{k\geqslant 2} > 0.5$, we consider the system as a dense system. A similar terminology is also used by Yates et al. [45] in a study of motion alignment in locusts which reports a connection between the frequency of transitions between stable states and the swarm density.

Fig. 1 shows three examples of node degree distributions based on Poisson distributions (eq. 1). These examples represent the three density classes as defined above (very sparse, sparse, dense). A very sparse system has a majority of agents either interacting with only one other agent (second-order interaction, node de-

[1] In appendix A, we provide an alternative approach to define swarm density based on areas.

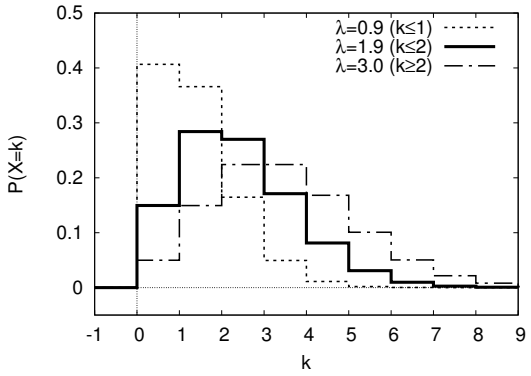

Fig. 1: Three examples of node degree distributions following Poisson distributions (eq. 1). With $\lambda = 0.9$ we have $P_{k\leqslant 1} > 0.5$ which indicates a very sparse system. With $\lambda = 1.9$ we have $P_{k\leqslant 2} > 0.5$ which indicates a sparse system. With $\lambda = 3$ we have $P_{k\geqslant 2} > 0.5$ which indicates a dense system.

gree $k = 1$) or none (node degree $k = 0$). A sparse system has a majority of agents either interacting with none, one, or two (third-order interactions) other agents (node degree $k \leqslant 2$). A dense system has a majority of agents interacting with two or more agents (node degree $k \geqslant 2$).

3.3 Second-order versus third-order interactions

We consider second-order interactions (node degree $k = 1$) and third-order interactions (node degree $k = 2$) as qualitatively different interaction patterns. A third-order interaction cannot be reduced to two second-order interactions because we assume reactive agents who do not keep memory of the past. Every agent must choose between two opinions, which we refer to as A and B. When two agents with different opinions meet, the symmetry is broken by either of the two at random. When three agents with differing opinions meet, a simple rule for agreement is for all the agents to pick the majority opinion. The convergence speed of the majority rule increases for an increasing number of agents involved in the decision process [42].

3.4 Well-mixed systems

A well-mixed system does not refer directly to the spatial distribution of agents and their absolute positions. Instead, with the term "well-mixed", we refer to the fact that each agent has the same probability to interact with any other agent in the swarm. The probability for an agent i to interact with an agent j is equal for all possible pairs of agents (i, j). More specifically, we refer to the absence of spatial correlations between agents with particular internal states. A well-mixed system has variance in its node degrees but the position of agents is independent of the agent's index or state.

3.5 Noise

In general, we can distinguish between two kinds of noise: intrinsic noise and extrinsic noise. Intrinsic noise originates from internal processes of the system, while extrinsic noise results from external factors, for example, from the environment. In this paper, we consider only intrinsic noise and we further categorize it into *agent* and *interaction* noise. In our study, agent noise is the result of spontaneous switching and represents an autonomous decision of the agent to change its internal state. Interaction noise is due to agents sampling the global system state based on their local neighborhood. In the following analysis, we focus on the effects of noise that makes agents switch state spontaneously. We refer to this noise with the term 'agent noise' while we use the term 'finite-size effects' to refer to interaction noise.

4 Models of very sparse, sparse, and dense swarms

In the following, we present three models of collective decision-making for very sparse, sparse and dense swarms, as described in Section 3.2. The second-order-interaction model represents interactions in very sparse swarms. The third-order-interaction model represents interactions in dense swarms. The intermediate model represents interactions in sparse swarms and combines the two other models to investigate a transition from second-order-interaction swarms to third-order-interaction

swarms. We choose chemical reactions as notation for these models and, in contrast to Biancalani et al. [4], we use discrete-time Markov chains to model our systems since they allow for a simpler derivation and analysis than stochastic differential equations.

4.1 The second-order-interaction model for very sparse swarms

Based on the Ohkubo system [29], Biancalani et al. [4] define a model of foraging in ants to investigate bistability. In their model, two food sources are present, and X_i denotes the number of ants foraging from source i. Recruitment is modeled such that ants foraging from one source recruit ants foraging from the other source. Ants are assumed to meet randomly in pairs. If they are foraging from different food sources—with equal probability—one of them switches to forage from the source of the other. This behavior is seen as autocatalytic recruitment [4] in analogy to chemical bistable systems [29]. In addition, the system is subject to agent noise, which is implemented as spontaneous switching. We model the foraging system using the chemical reaction network

$$\mathrm{X}_1 + \mathrm{X}_2 \xrightarrow{\mathrm{r}} 2\,\mathrm{X}_1, \tag{5}$$

$$\mathrm{X}_2 + \mathrm{X}_1 \xrightarrow{\mathrm{r}} 2\,\mathrm{X}_2, \tag{6}$$

$$\mathrm{X}_1 \xrightarrow{\varepsilon} \mathrm{X}_2, \tag{7}$$

$$\mathrm{X}_2 \xrightarrow{\varepsilon} \mathrm{X}_1, \tag{8}$$

where the constants r and ε are the reaction rate coefficients, respectively, r for recruitment and ε for spontaneous switching. Whenever ants with different sources meet, either reaction 5 or 6 is executed, with equal probability. We argue that this model can be interpreted as a model for very sparse swarms.

In contrast to Biancalani et al. [4], we use a Markov chain model to compute stationary distributions and mean first passage times (MFPT) of the second-order-interaction model. First, we introduce the swarm fractions x_1 and x_2 to represent the fraction of agents in a swarm of size N for each of the two types X_1 and X_2 ($x_1 + x_2 = 1$). The use of swarm fractions allows us to derive the transition probabilities under the continuous limit approximation (see Biancalani et al. [4]). The transition

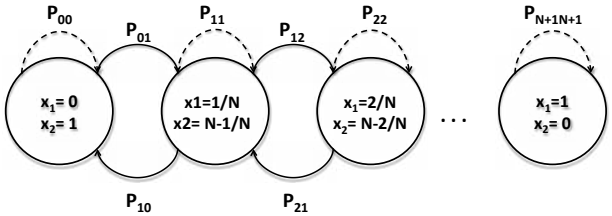

Fig. 2: Markov chain to model the collective decision-making system.

probabilities of the chemical reaction network (eqs. 5 to 8) are

$$\begin{aligned} T_1 &\equiv T\left(x_1 + \frac{1}{N}, x_2 - \frac{1}{N}\middle| x_1, x_2\right) = rx_1x_2 + \varepsilon x_2, \\ T_2 &\equiv T\left(x_1 - \frac{1}{N}, x_2 + \frac{1}{N}\middle| x_1, x_2\right) = rx_1x_2 + \varepsilon x_1, \end{aligned} \tag{9}$$

for $r \leqslant 1$ and $\varepsilon \leqslant 1$, T_1 is the probability of observing a switch from X_2 to X_1 and T_2 is the probability of a switch from X_1 to X_2 [4].

We define a Markov chain of $N+1$ states and their respective transitions under the assumption of observing only one switch at a time as shown in Fig. 2. The non-zero transition probabilities of the defined Markov chain are given based on the transition probabilities in eq. (9):

$$\begin{aligned} p_{i,i+1} &= rx_1x_2 + \varepsilon x_2, \\ p_{i,i-1} &= rx_1x_2 + \varepsilon x_1, \\ p_{i,i} &= 1 - (rx_1x_2 + \varepsilon x_2 + rx_1x_2 + \varepsilon x_1), \end{aligned} \tag{10}$$

with $p_{i,i+1}$ defining the probability of transitions that increase the number of agents of type X_1, $p_{i,i-1}$ defining the probability of transitions that decrease the number of agents of type X_1, and $p_{i,i}$ giving the probability of staying in the current state.

4.2 The third-order-interaction model for dense swarms

As a high-density complement to the second-order-interaction model, we define a model that requires three ants to meet at a place for recruitment [14]. In this model, the majority rule [8, 1, 28, 42] can be used to convince the minority forager

to change its opinion. We model the foraging system using the chemical reaction network

$$2\,\mathrm{X}_1 + \mathrm{X}_2 \xrightarrow{\mathrm{r}} 3\,\mathrm{X}_1, \tag{11}$$

$$\mathrm{X}_1 + 2\,\mathrm{X}_2 \xrightarrow{\mathrm{r}} 3\,\mathrm{X}_2, \tag{12}$$

$$\mathrm{X}_1 \xrightarrow{\varepsilon} \mathrm{X}_2, \tag{13}$$

$$\mathrm{X}_2 \xrightarrow{\varepsilon} \mathrm{X}_1, \tag{14}$$

with reaction rate coefficients r for recruitment and ε for spontaneous switching. The interaction graph has consequently a maximal node degree of two. Such a small node degree barely justifies calling the modeled swarm "dense", however, this model should be seen as a representation of swarm systems implementing a majority rule for any node degree bigger than one ($k \geqslant 2$). Systems with bigger node degrees only differ quantitatively in their convergence speed [14].

Similarly to the second-order model, we apply the continuous limit approximation for determining the transition probabilities. The continuous limit approximation is particularly useful in this case as it allows us to ignore the order of agents involved in the majority decision and to simplify our derivations (see Dyson et al. [7]). The transition probabilities of the chemical reaction network (eqs. 11 to 14) are

$$\begin{aligned} T_1 &\equiv T\left(x_1 + \frac{1}{N}, x_2 - \frac{1}{N}\middle| x_1, x_2\right) = r x_1^2 x_2 + \varepsilon x_2, \\ T_2 &\equiv T\left(x_1 - \frac{1}{N}, x_2 + \frac{1}{N}\middle| x_1, x_2\right) = r x_1 x_2^2 + \varepsilon x_1. \end{aligned} \tag{15}$$

Hence, the Markov chain probabilities for the third-order-interaction model for $r \leqslant 1$ and $\varepsilon \leqslant 1$ are defined as

$$\begin{aligned} p_{i,i+1} &= r x_1^2 x_2 + \varepsilon x_2, \\ p_{i,i-1} &= r x_1 x_2^2 + \varepsilon x_1, \\ p_{i,i} &= 1 - (r x_1^2 x_2 + \varepsilon x_2 + r x_1 x_2^2 + \varepsilon x_1). \end{aligned} \tag{16}$$

4.3 The intermediate model for sparse swarms

Finally, we define an intermediate model to represent any combination of the second-order-interaction model and the third-order-interaction model. The intermediate model is formed by the recruitment reactions for node degree $k = 1$ and $k = 2$, as well as by the reactions implementing spontaneous switching. Thus, it is an appropriate model to address the variance of node degrees that causes variations in local swarm densities. The chemical reaction network of the intermediate model is given by

$$\mathrm{X}_1 + \mathrm{X}_2 \xrightarrow{\mathrm{r}_1} 2\,\mathrm{X}_1, \tag{17}$$

$$\mathrm{X}_2 + \mathrm{X}_1 \xrightarrow{\mathrm{r}_1} 2\,\mathrm{X}_2, \tag{18}$$

$$2\,\mathrm{X}_1 + \mathrm{X}_2 \xrightarrow{\mathrm{r}_2} 3\,\mathrm{X}_1, \tag{19}$$

$$\mathrm{X}_1 + 2\,\mathrm{X}_2 \xrightarrow{\mathrm{r}_2} 3\,\mathrm{X}_2, \tag{20}$$

$$\mathrm{X}_1 \xrightarrow{\varepsilon} \mathrm{X}_2, \tag{21}$$

$$\mathrm{X}_2 \xrightarrow{\varepsilon} \mathrm{X}_1, \tag{22}$$

for reaction rate coefficient r_1 for recruitment in groups of size two, reaction rate coefficient r_2 for recruitment in groups of size three, and reaction rate coefficient ε for spontaneous switching.

From the chemical reactions (eq. 17 to 22) we can determine the transition probabilities

$$\begin{aligned} T_1 &\equiv T\left(x_1 + \frac{1}{N}, x_2 - \frac{1}{N}\middle| x_1, x_2\right) = r_2 x_1^2 x_2 + r_1 x_1 x_2 + \varepsilon x_2, \\ T_2 &\equiv T\left(x_1 - \frac{1}{N}, x_2 + \frac{1}{N}\middle| x_1, x_2\right) = r_2 x_1 x_2^2 + r_1 x_1 x_2 + \varepsilon x_1, \end{aligned} \tag{23}$$

for $r_1, r_2 \leqslant 1$ and $\varepsilon \leqslant 1$. This defines a Markov chain model that allows us to explore a continuum of swarm densities by varying the ratio between rate coefficients r_1 and r_2. That is, we vary the probabilities of an agent to interact with either one or two neighbors[2]. For example, if most agents have a node degree of $k = 1$ then the probability $P(X = 1)$ is the highest among the other probabilities (i.e., agents are

[2] As defined in Section 3.2, sparse systems have a majority of nodes with degree two or less: $P(X = 0) + P(X = 1) + P(X = 2) > 0.5$.

meeting mostly in pairs). This leads to a reaction rate coefficient r_1 that is higher than both r_2 and ε. Similarly, if the system is denser and mostly three agents are meeting, then the reaction rate coefficient r_2 is increased to be greater than both r_1 and ε. If we assume to have a constant ε, the relation between r_1 and r_2 allows us to define a system density measure over a continuous range

$$d = r_2 - r_1, \tag{24}$$

that we will use later in Sec. 5.3.

Finally, we derive the transition probabilities of the Markov chain to explore a continuum of swarm densities by varying the ratio of the rate coefficients r_1 and r_2:

$$\begin{aligned} p_{i,i+1} &= r_2 x_1^2 x_2 + r_1 x_1 x_2 + \varepsilon x_2, \\ p_{i,i-1} &= r_2 x_1 x_2^2 + r_1 x_1 x_2 + \varepsilon x_1, \\ p_{i,i} &= 1 - (r_2 x_1^2 x_2 + r_1 x_1 x_2 + \varepsilon x_2 + r_2 x_1 x_2^2 + r_1 x_1 x_2 + \varepsilon x_1). \end{aligned} \tag{25}$$

5 Results

In the following, we give examples for the three models described in the previous section. We describe conditions for noise-induced bistability in the second-order-interaction model, we compute mean first passage times (MFPT), which can be helpful to determine critical population sizes experimentally, and we investigate the intermediate model in particular.

5.1 The second-order-interaction model for very sparse swarms

As done by Biancalani et al. [4], we define the system state as $z = x_1 - x_2$, $z \in [-1, 1]$. This swarm system displays noise-induced bistability: "This type of bistability cannot be understood from the fixed points of the corresponding deterministic [differential] equations" [4] because the expected change of z is $dz/dt = -\varepsilon z$ for the infinite limit $N \to \infty$. This defines a negative feedback process and has

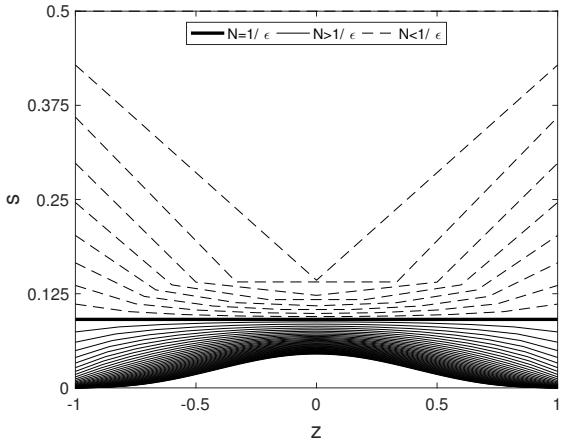

Fig. 3: the label of y-axis is corrected.
Second-order-interaction model: stationary distribution for different swarm sizes $N \in [1, 50]$. In the figure are shown: sub-critical ($N < 1/\varepsilon$, dashed lines), critical ($N = N_c = 1/\varepsilon$, thick line), and super-critical sizes ($N > 1/\varepsilon$, continuous lines) for $\varepsilon = 1/10$. Note the bimodal (U-shape, dashed lines) and unimodal (inverted U-shape, continuous lines) distributions.

a stable fixed point at $z^* = 0$ [4]. Depending on the rate coefficient ε, we define a critical swarm size $N_c = 1/\varepsilon$ [4], such that the system is bistable for $N < N_c$ (i.e., bimodal stationary distributions) and unistable for $N \geqslant N_c$ (i.e., unimodal stationary distributions). It is important to note that noise-induced bistable systems such as the systems modeled using the second-order-interaction model do not scale well due to the existence of a critical swarm size.

We use standard numerical techniques to compute the stationary distribution s of the Markov chain given by the transition probabilities in eq. 10. The resulting distribution is shown in Fig. 3 for three parameter settings: $N < 1/\varepsilon$, $N = N_c = 1/\varepsilon$, and $N > 1/\varepsilon$. For $N < 1/\varepsilon$, the model converges to bimodal distributions and models therefore an effective decision-making system (i.e., the system resides for most of the time in the extreme states of $z = -1$ and $z = 1$). For $N > 1/\varepsilon$, the model converges to unimodal distributions and thus models a system that fails to make a collective decision (i.e., the system resides for the most time in "undecided" states close to $z = 0$).

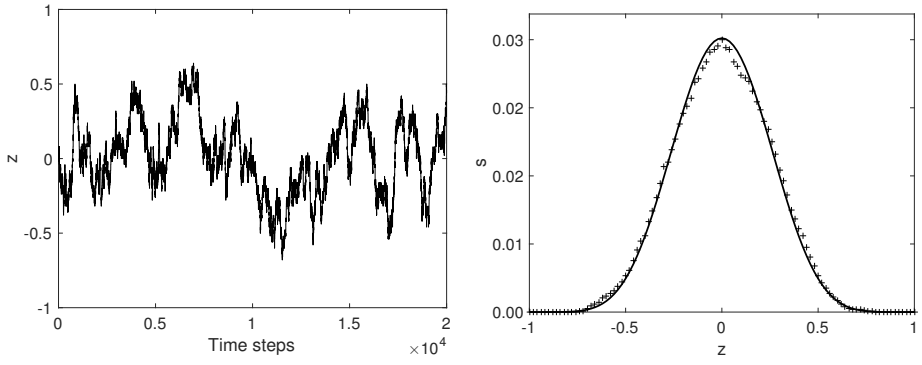

(a) (b)

Fig. 4: Second-order-interaction model (eqs. 5 to 8): the case of $N > 1/\varepsilon$. (a) A trajectory of $z = x_1 - x_2$ sampled from the Markov chain. (b) The stationary distribution of z compared to the average of 50 data samples (parameter setting: $\varepsilon = 1/10$, $r = 1$, $N = 100$).

Next, we show a few trajectories of z that we directly sample from the Markov chain model. We initialize the system to $\mathbf{X} = (X_1, X_2) = (N/2, N/2)$, which corresponds to $\mathbf{x} = (0.5, 0.5)$ and $z = 0$. The rate coefficient r is set to $r = 1$.

We start with the super-critical situation of $N > \frac{1}{\varepsilon}$ ($N\varepsilon > 1$, $\frac{1}{\varepsilon} = N_c = 10$). Parameters are set to $\varepsilon = \frac{1}{10}$, $r = 1$, and $N = 100$. Fig. 4a shows a trajectory of z sampled from the Markov chain, in which the system fluctuates around $z = 0$. Fig. 4b shows the respective unistable stationary distribution obtained from the Markov model (eq. 10). The stationary distribution is compared to data obtained from 50 samples of the Markov chain.

To trigger a sub-critical situation of $N < \frac{1}{\varepsilon}$ ($N\varepsilon < 1$, $\frac{1}{\varepsilon} = N_c = 100$) we set $\varepsilon = \frac{1}{100}$, $r = 1$, and $N = 50$. Fig. 5a shows a trajectory of z sampled from the Markov chain, in which the system stays close to either $z = 1$ or $z = -1$ for most of the time and switches between them relatively frequently. Fig. 5b shows the respective bistable stationary distribution of z. The stationary distribution is compared to data obtained from 50 samples from the Markov chain.

An interesting feature of the stationary distribution is the expected time to switch from one stable state to the other. This value is an indicator of how the system approaches the exploitation vs exploration tradeoff. A short switching time (i.e., high switching frequency) indicates a high degree of exploration and thus a certain readiness for dynamic changes in the environment. A long switching time

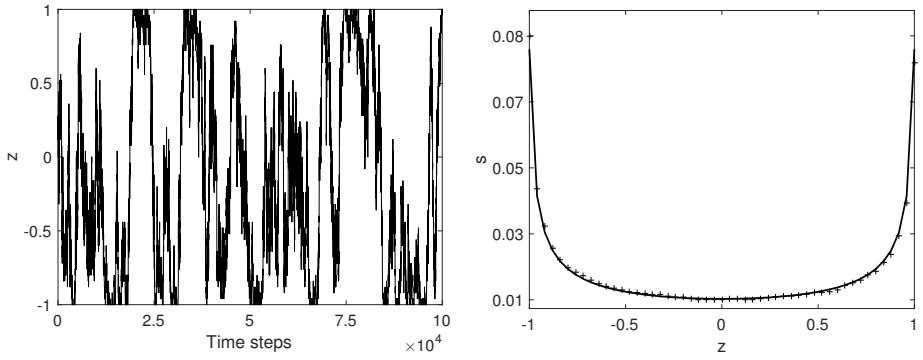

(a) (b)

Fig. 5: Second-order-interaction model (eqs. 5 to 8): the case of $N < 1/\varepsilon$. (a) A trajectory of $z = x_1 - x_2$ sampled from the Markov chain. (b) The stationary distribution of z compared to the average of 50 data samples (parameter setting: $\varepsilon = 1/100$, $r = 1$, $N = 50$).

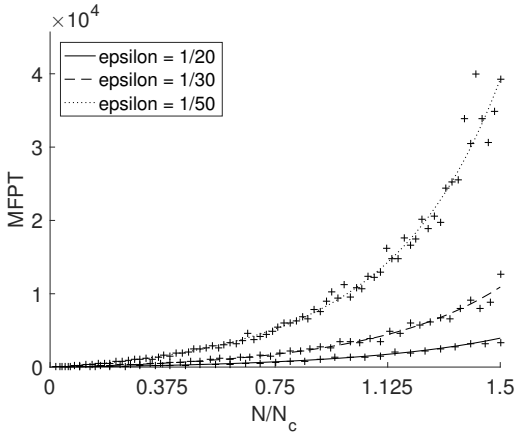

Fig. 6: Second-order-interaction model (eqs. 5 to 8): mean first passage times (MFPT) from one stable state to the other. The figure shows the Markov model (solid, dashed and dotted lines) compared to data from 100 samples of the Markov chain (crosses) (parameter settings: $\varepsilon \in \{\frac{1}{20}, \frac{1}{30}, \frac{1}{50}\}$ and $N_c = 1/\varepsilon$).

(i.e., low switching frequency) indicates a high degree of exploitation. We are interested in the MFPT between the two stable (boundary) states given by[3]

$$m_{0,N} = \frac{f_{N,N} - f_{0,N}}{s_N}, \tag{26}$$

Where $f_{i,j}$ is the expected number of visits to state j starting from state i.

[3] See Appendix B

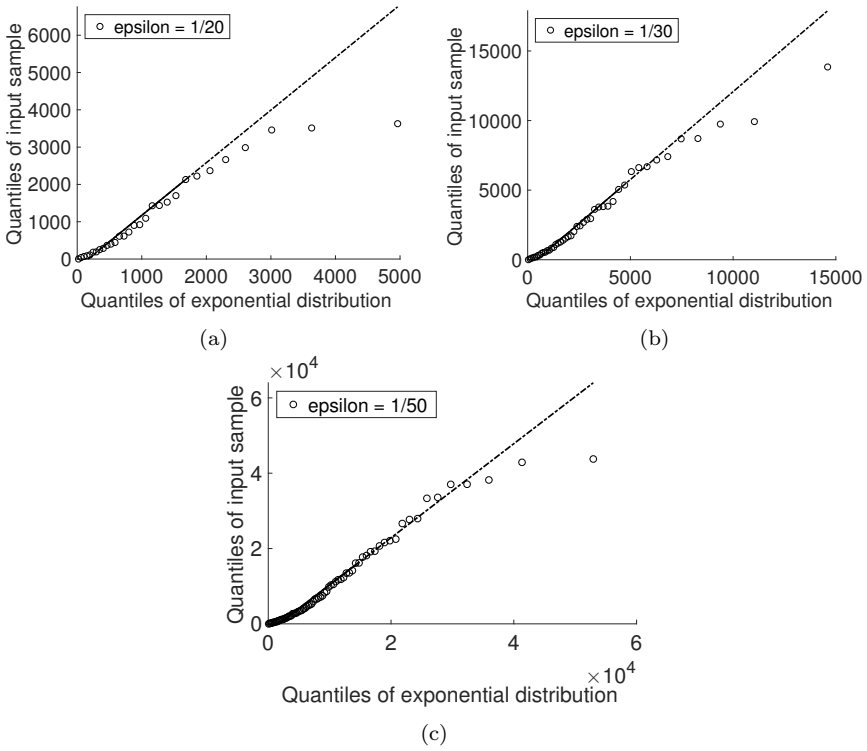

Fig. 7: Analysis of the mean first passage times (MFPT) for the second-order-interaction model. Quantile-quantile plots of the data are obtained from simulations for (a) $\varepsilon = \frac{1}{20}$, (b) $\varepsilon = \frac{1}{30}$, and (c) $\varepsilon = \frac{1}{50}$ and compared to an exponential distribution.

In Fig. 6 we show the MFPT computed according to eq. 26. We compare it to data of 100 samples from the Markov chain for parameters $\varepsilon \in \{\frac{1}{20}, \frac{1}{30}, \frac{1}{50}\}$ and $N/N_c \in [0, 1.5]$. The calculated value and the Markov chain simulation match, and the MFPT grows exponentially with $\frac{N}{N_c}$. To verify exponential scaling, we used a quantile-quantile (q-q) plot of the data obtained from the simulations against an exponential distribution as shown in Fig. 7. The symbols in the q-q plot lay on a straight line indicating a linear correlation between the data and the exponential distribution. However, the values are off the main diagonal indicating a linear deviation from the exponential distribution (slopes: 1.41 for $\varepsilon = \frac{1}{20}$, 1.26 for $\varepsilon = \frac{1}{30}$, and 1.25 for $\varepsilon = \frac{1}{50}$). Additionally, for large MFPT, we can observe a more systematic deviation from the straight line indicating that the distribution of our data is skewed. We tested our data against an exponential distribution with a one-

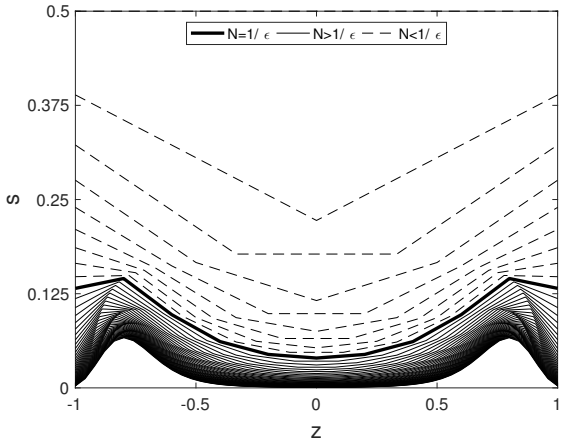

Fig. 8: Third-order-interaction model: stationary distribution for different swarm sizes N. Note that for any setting we get a bimodal distribution.

sample Kolmogorov-Smirnov test. The null hypothesis that the sample is drawn from an exponential distribution could not be rejected (p-values: 0.93 for $\varepsilon = \frac{1}{20}$, 0.75 for $\varepsilon = \frac{1}{30}$, and 0.20 for $\varepsilon = \frac{1}{50}$). Therefore, we conclude that the data are approximately exponentially distributed. A long MFPT means that the system switches infrequently between the stable states and has thus a limited adaptivity to changes in the environment. From this discussion, we conclude that adaptivity scales poorly with the number of agents.

5.2 The third-order-interaction model for dense swarms

For the third-order-interaction model there is no critical swarm size N_c. The foraging system is always bistable unless it is dominated by agent noise. Hence, it shows a bimodal stationary distribution for a large enough swarm size N and is scalable. We compute the stationary distribution s of the Markov chain given by the transition probabilities in eq. 16. The resulting stationary distribution s is shown in Fig. 8 for three parameter settings: $N < 1/\varepsilon$, $N = 1/\varepsilon$, and $N > 1/\varepsilon$. For all tested settings we obtain bistable distributions with the only difference that, for $N > 1/\varepsilon$, the stable states shift slightly away from the boundaries $z = -1$ and $z = 1$ due to the effect of spontaneous switching.

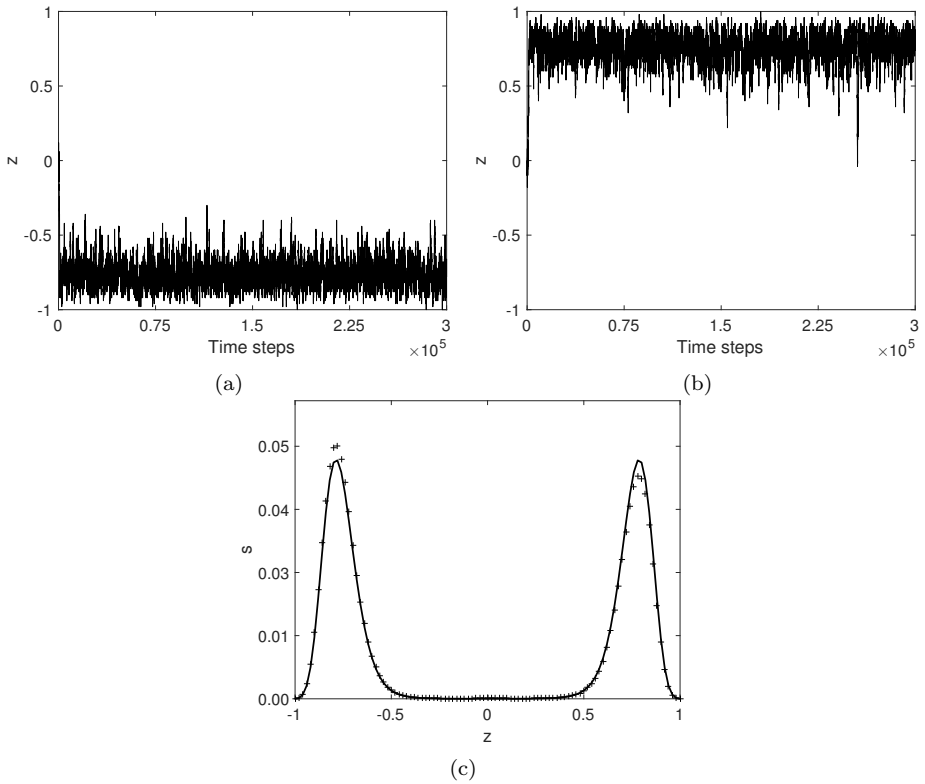

Fig. 9: Third-order-interaction model (eqs. 11 to 14). (a,b) Two trajectories of $z = x_1 - x_2$ sampled from the Markov chain. (c) The stationary distribution of z compared to the average of 50 data samples (parameter setting: $\varepsilon = 1/10$, $r = 1$, $N = 100$).

We show in Figs. 9a and b a few trajectories of z sampled directly from the Markov chain of the third-order-interaction model. The system stays either close to $z \approx 0.79$ or $z \approx -0.79$ for most of the time. The system switches infrequently between stables states because of its relatively big size. Fig. 9c shows the respective stationary distribution obtained from the Markov model (eq. 16).

We test a lower noise-level for the third-order-interaction model by setting $\varepsilon = \frac{1}{100}$. Figs. 10a and b show sample trajectories of z. The system stays close to either $z = 1$ or $z = -1$ for most of the time and still switches infrequently between the stable states because of its relatively big size. Fig. 10c shows the respective stationary distribution of z.

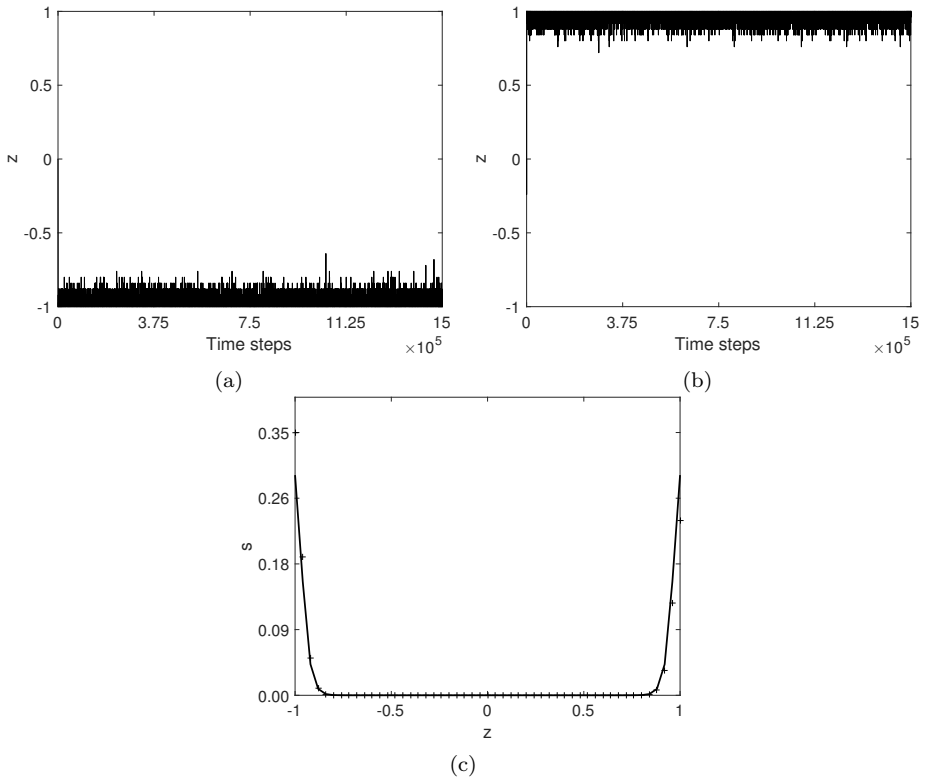

Fig. 10: Third-order-interaction model (eqs. 11 to 14). a) and b) Two trajectories of $z = x_1 - x_2$ sampled from the Markov chain. c) The stationary distribution of z compared to the average of 50 data samples (parameter settings: $\varepsilon = 1/100$, $r = 1$, $N = 50$).

In Fig. 11 we show the MFPT computed for the Markov chain according to eq. 26 and we compare it to data from 100 samples from the Markov chain for parameters $\varepsilon \in \{1/20, 1/30\}$ and $N \in \{1, 2, \ldots, 45\}$. Again, the MFPT increases approximately exponentially with the swarm size and hence shows that adaptivity scales badly. A quantitative comparison with Fig. 6 indicates that the second-order-interaction model has an MFPT that is magnitudes smaller than that of the third-order-interaction model (e.g., for $N = 45$, $\varepsilon = \frac{1}{30}$, magnitude of 10^4 for the second-order-interaction model compared to 10^7 for the third-order-interaction model).

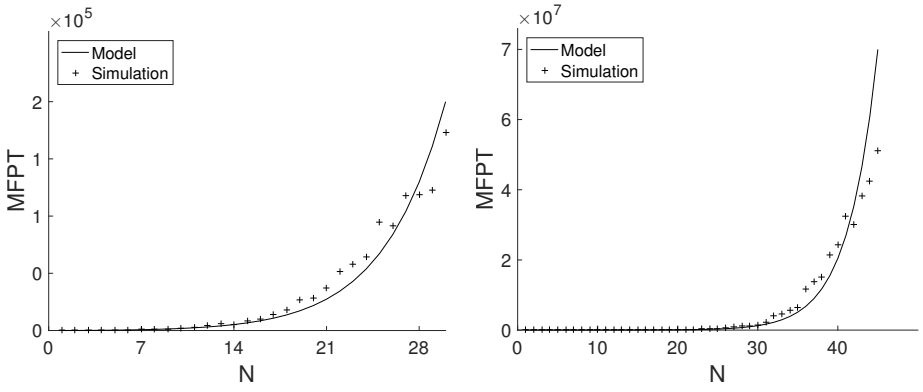

(a) (b)

Fig. 11: Mean first passage times (MFPT) from one stable state to the other for the third-order-interaction model (eqs. 11 to 14). (a) For the parameter settings: $\varepsilon = 1/20$ and $N \in \{1, 2, \ldots, 30\}$. (b) For the parameter settings $\varepsilon = 1/30$ and $N \in \{1, 2, \ldots, 45\}$, Markov model (solid line) compared to 100 data samples (crosses).

5.3 The intermediate model for sparse swarms

We investigate the influence of varying densities using the intermediate model defined in eqs. 17 to 22. We use this model for sparse swarms whose observed node degrees are mostly $k = 0$, $k = 1$, and $k = 2$. Depending on the chances of each node degree to appear, we configure the corresponding reaction rate coefficient. We model the different interaction probabilities in two ways. We can vary simultaneously the value of both the recruitment rates r_1, r_2 and the spontaneous switching rate ε. Alternatively, we can keep the value of ε constant and vary only the values of r_1 and r_2. We distinguish between the three cases *(i)* when agents tend to have no neighbors in range, spontaneous switching (eqs. 21 and 22) occurs with the highest probability. Hence, this system is dominated by agent noise and can be modeled by $\varepsilon/r_1 \gg 1$ and $\varepsilon/r_2 \gg 1$. A resulting stationary distribution is shown in Fig. 12a, in which we can notice that the system is unistable due to the high degree of agent noise; *(ii)* when the agents tend to have one or no neighbors, we discriminate between *noisy* and *non-noisy* systems. In a noisy system, spontaneous switching (eqs. 21 and 22) as well as pairwise reactions (eqs. 17 and 18) are frequent; whereas, in a non-noisy system only pairwise reactions (eqs. 17 and 18) have a high reaction rate coefficient. This system can be noise-induced bistable de-

pending on its size and on whether it is dominated by agent noise. The stationary distribution of a unistable system is shown in Fig. 12b. The stationary distribution of a noise-induced bistable system is shown in Fig. 12c; *(iii)* when most of the agents have at least two neighbors, we again distinguish between noisy and non-noisy systems. In a noisy system, all reactions have about the same frequency. In contrast, in a non-noisy system, the multi-fold (in our case third-order) reactions (eqs. 19 and 20) have the highest reaction rate coefficient. This system can be unistable or bistable depending on whether it is dominated by agent noise or not. The stationary distribution of a unistable system is shown in Fig. 12d. The stationary distribution of a bistable system is shown in Fig. 12e. We can represent these three cases of the system by choosing appropriate values for the reaction rate coefficients r_1, r_2, and ε in the intermediate model.

6 Density independent of noise

Finally, we consider a model with constant, density-independent agent noise; This could be observed in collective decision-making systems in which the decision of an agent to switch opinion spontaneously is taken individually and independently. Using such a model allows us to focus on studying the dynamics of the swarm for varying density as defined in eq. 24. Hence, we set the reaction rate coefficient $\varepsilon = 0.1$ for spontaneous switching and the reaction rate coefficients r_1 and r_2 are varied but restricted to $r_1, r_2 \in [0, 1]$ and $r_1 + r_2 = 1$. We use the density parameter $d = r_2 - r_1$ as defined in eq. 24 that allows us to emulate different swarm densities. For $d = -1$ we get a second-order-interaction model, for $d = 1$ we get a third-order-interaction model, and for increasing density d from $d = -1$ to $d = 1$ we can investigate the transition from one model to the other. We rewrite the transition probabilities from eq. 25 by substituting d for r_1 and r_2:

$$
\begin{aligned}
p_{i,i+1} &= \frac{d-1}{2} x_1^2 x_2 + \frac{1+d}{2} x_1 x_2 + \varepsilon x_2, \\
p_{i,i-1} &= \frac{d-1}{2} x_1 x_2^2 + \frac{1+d}{2} x_1 x_2 + \varepsilon x_1, \\
p_{i,i} &= 1 - \left(\frac{d-1}{2} x_1^2 x_2 + \frac{1+d}{2} x_1 x_2 + \varepsilon x_2 + \frac{d-1}{2} x_1 x_2^2 + \frac{1+d}{2} x_1 x_2 + \varepsilon x_1 \right). \quad (27)
\end{aligned}
$$

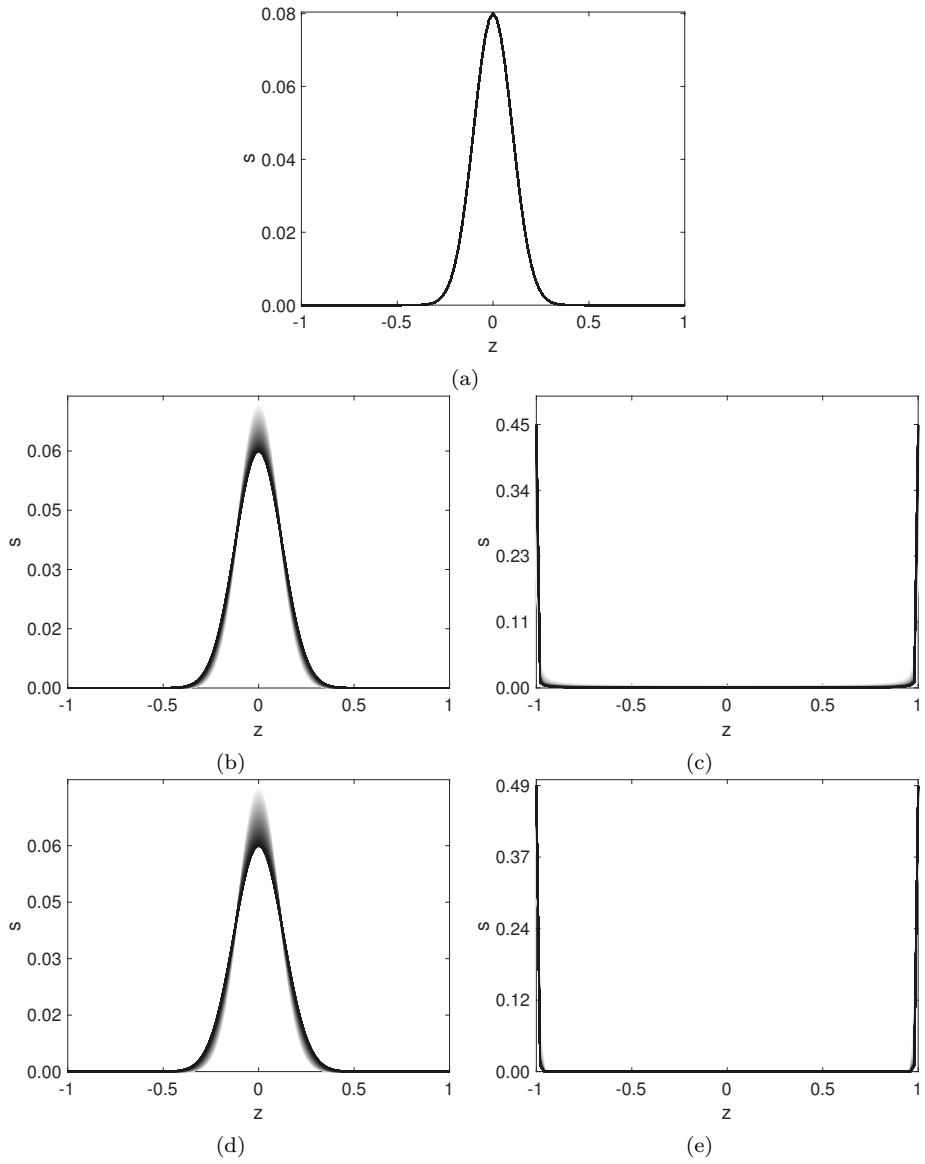

Fig. 12: Stationary distributions for different densities (very sparse, sparse, dense) in the intermediate model. Parameter settings: $N = 100$, (a) $\varepsilon \in [0.005, 0.05]$, $r_1 = 10^{-5}$, $r_2 = 10^{-5}$. (b) $\varepsilon = 0.05$, $r_1 \in [0.005, 0.05]$, $r_2 = 10^{-5}$. (c) $\varepsilon = 10^{-5}$, $r_1 \in [0.005, 0.05]$, $r_2 = 10^{-5}$. (d) $\varepsilon = 0.05$, $r_1 = 0.05$, $r_2 \in [0.005, 0.05]$. (e) $\varepsilon = 10^{-5}$, $r_1 = 0.05$, $r_2 \in [0.005, 0.05]$

In Fig. 13 we show the stationary distributions of the model computed for a varying swarm density d over the full range $[-1, 1]$ (in steps of 0.001). Both the

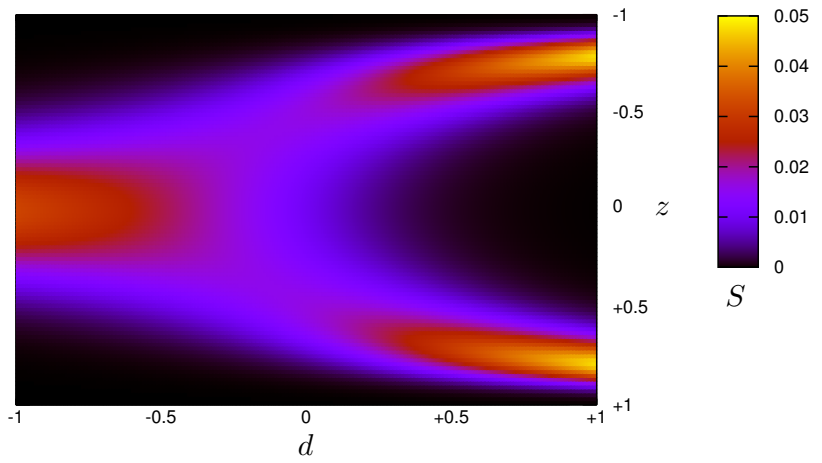

Fig. 13: Intermediate model: stationary distributions for varied swarm density $d \in [-1, 1]$. The bifurcation point is $d^* \approx -0.232$, $d = r_2 - r_1$, $r_1 + r_2 = 1$, $\varepsilon = 0.1$, $N = 100$, warm colors represent high probabilities, cold colors represent low probabilities.

agent noise level ($\varepsilon = 0.1$) and the swarm size $N = 100$ are chosen such that the intermediate model does not show noise-induced bistability. Consequently, Fig. 13 shows a unistable distribution for $-1 \leqslant d < -0.232$. By increasing the density from $d = -1$ to $d \approx -0.232$, the state of the swarm has an unistable distribution which covers a wider range of z-values centered around $z = 0$; starting from $d^* \approx -0.232$ the swarm makes a transition to a bistable distribution due to the influence of the majority rule reactions outplaying spontaneous switching. Thus, the approximate bifurcation point is $d^* \approx -0.232$. This situation can be interpreted as a stochastic variant of a super-critical pitchfork bifurcation, that is, a random dynamical attractor [2] emerges as a consequence of the positive feedback generated by the application of the majority rule. This can be explained by the following consideration. The effect of the majority rule is modeled by the term $rz(1-z^2)/2$ [14] and the normal form of a super-critical pitchfork bifurcation is a similar polynomial that differs only in its constants: $dz/dt = cz - z^3$.

In summary, we notice a strong dependency of the collective decision-making system on the swarm density. Such a dependency has a qualitative impact and can turn a fully effective system (i.e., a bistable system that resides most of the

time close to one of the two consensus decisions) into an ineffective system (i.e., a unistable system that is most of the time far from a consensus decision).

7 Agent-based simulations

To validate the theoretical results discussed so far and reveal the effect that space aspects have on the dynamics of the decision-making process, we performed a further set of experiments with an agent-based model of our system[4].

The two salient features of the mathematical model are *(i)* that the system is assumed well-mixed, and *(ii)* the agents make decisions depending on the number of neighbors they encounter. To account for *(i)*, we considered agents as point-masses characterized by position and velocity, and we let the agents move randomly in the environment. We identified two ways to allow the system to mix well: setting the maximum speed of the agents and tuning the frequency of the decisions. Regarding *(ii)*, since the agents are moving, fixing a specific node-degree-based density is not possible, and the system will have a mix of second- and third-order interactions. However, it is possible to favor either type of interaction by considering the spatial density of the agents, defined as the ratio between the total area occupied by the agents' communication range and the total area of the environment. Intuitively, low-density simulations (in the spatial sense) correspond to cases in which the dynamics is dominated by agents having zero or one neighbor at most; differently, with high spatial density the dynamics is dominated by agents with two or more neighbors.

The behavior of each agent is formalized in Alg. 1. Every agent is characterized by its position $\mathbf{p}$, its velocity $\mathbf{v}$, and its current decision d. The simulation proceeds in a step-wise fashion, and t indicates the current step. The agent updates its position at every step, and makes a decision every T steps (in a synchronous fashion). When making a decision, the agent considers the number of its neighbors: if no neighbor is around, the agent switches with probability ε; with exactly one neighbor, it switches with probability r_1 if the neighbor disagrees with the agent; with two or more neighbors, the agent switches with probability r_2 if it is in

[4] The source code of the agent-based simulator can be downloaded at: https://github.com/NESTLab/DMSim

Algorithm 1 The decision-making algorithm followed in our agent-based simulations discussed in Sec. 7. The agent is characterized by position $\mathbf{p}$, velocity $\mathbf{v}$, and current decision d. The maximum speed is calculated as a fraction M of the environment side length L.

```
if t mod T = 0 then                                   ▷ This is a decision step
    v ← ML[U(−1,1),U(−1,1)]                           ▷ Random speed
    n ← number of neighbors
    if n = 0 then                                     ▷ No neighbors
        d ← switch(d, ε)                              ▷ Switch decision with prob ε
    else if n = 1 then                                ▷ Exactly one neighbor
        if neighbor has different choice then
            d ← switch(d, r1)                         ▷ Switch decision with prob r1
    else if n = 2 then                                ▷ Exactly two neighbors
        if both neighbors have different choice from this agent then
            d ← switch(d, r2)                         ▷ Switch decision with prob r2
    else                                              ▷ More than two neighbors
        Pick two neighbors at random
        if both neighbors have different choice from this agent then
            d ← switch(d, r2)                         ▷ Switch decision with prob r2
p ← update(p, v)                                      ▷ Update agent pose and solve collisions
```

a minority decision with respect to the other two neighbors, see eq. (11) and eq. (12). Every decision step, the agent also picks a new random velocity vector. Rather than fixing the speed throughout the entire run, this choice simulates better the possible behavior of the agents in a real setting, and prevents the creation of recurring motion patterns that could skew the results.

At the beginning of each experimental run, $N = 100$ agents are uniformly distributed in the environment. The environment is a square with side length L, a screenshot of our agent-based simulator is shown in Fig. 14. Whenever an agent is about to move past the environment boundaries, its velocity is fixed to make it "bounce" against the wall, preventing it from leaving the arena. By controlling the size of the arena, we can control the spatial density of the robots. More specifically, given a certain spatial density δ that we aim to impose, the side of the square environment is calculated as $L = \sqrt{N\pi/\delta}$. To account for mixing, in our experiments we set the maximum speed a robot can travel as a fraction M of the environment side length (i.e., maximum speed is ML). This choice allows us to compare experimental setups with different spatial densities, and assess the effect of the agent speed on the decision-making process. Finally, we set the decision

frequency $1/T = 0.1$, that is, the robots make a decision every 10 time steps. To collect meaningful statistics, each setup $\langle \varepsilon, r_1, r_2, \delta, M \rangle$ was run 100 times.

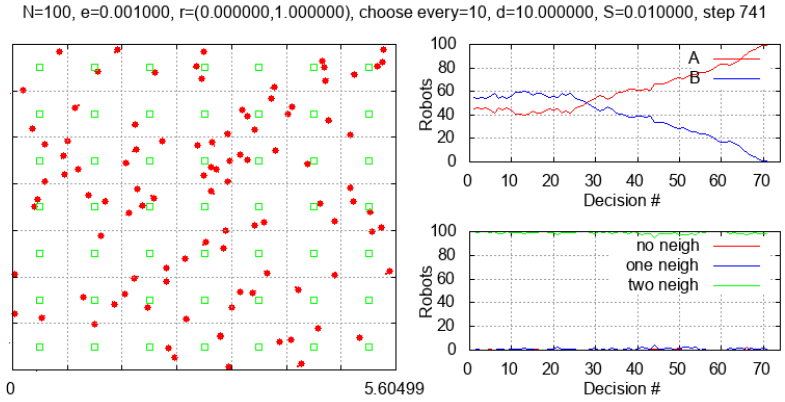

Fig. 14: A screenshot of the agent-based simulator at simulation step 741.

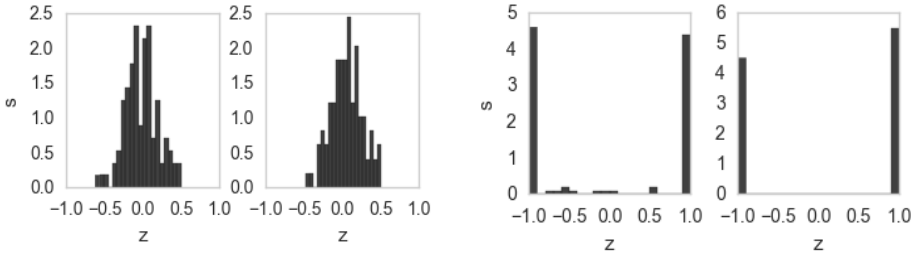

(a) (b)

Fig. 15: Second-order model (very sparse system) with $N = 100$ and $\delta = 0.1$. (a) $1/\varepsilon = 10$ ($N > 1/\varepsilon$), maximum speed is 0.01 left and 0.1 right. (b) $1/\varepsilon = 1000$ ($N < 1/\varepsilon$), maximum speed is 0.01 left and 0.1 right.

The results of our experiments are reported in Figs. 15–17. Fig. 15 shows how the second-order model, which corresponds to a very sparse agent distribution, agrees with the mathematical model dynamics shown in Figs. 4 and 5. This holds both for the case $N > 1/\varepsilon$ and $N < 1/\varepsilon$, regardless of the value of the maximum speed ML, $M \in \{0.01, 0.1\}$. Fig. 16 shows the behavior of the third-order model,

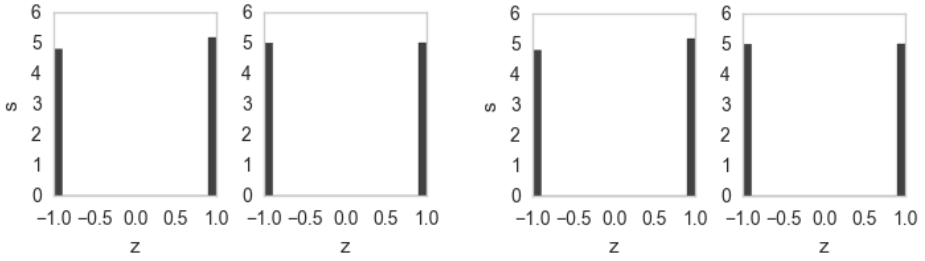

Fig. 16: Third-order model (dense system) with $N = 100$ and $\delta = 10$. (a) $1/\varepsilon = 10$ ($N > 1/\varepsilon$), maximum speed is 0.01 left and 0.1 right. (b) $1/\varepsilon = 1000$ ($N < 1/\varepsilon$), maximum speed is 0.01 left and 0.1 right.

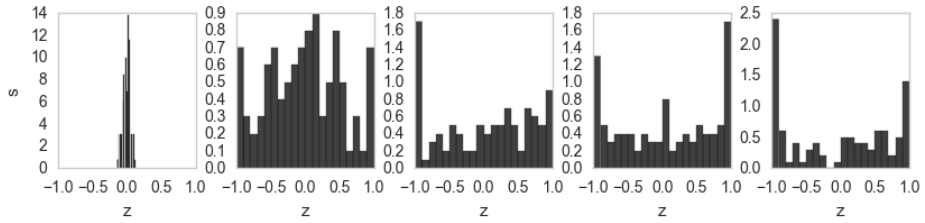

Fig. 17: The agent density independent of noise. Density here is defined as $r_2 - r_1$ (see Sec. 6). It is independent of the agent noise ε. We set $N = 100$, $1/\varepsilon = 10$, maximum speed $= 0.001$, and $r_1 - r_2 = [-1, 0.5, 0, 0.5, 1]$ from left to right.

which corresponds to a dense swarm. Also in this case the results match the mathematical model regardless of the maximum speed—the system stays decided, see Fig. 9 and 10. Finally, the graphs in Fig. 17 show that the bifurcation predicted by our mathematical model (see Fig. 13) are confirmed also with agent-based simulations. We have selected a low value for the maximum speed (i.e., $M = 0.001$), so that the switch of the system from being undecided to being decided can be observed smoothly (other values of maximum speed show qualitatively the same behavior but it is not so easily observed).

8 Discussion and conclusion

We have presented two mathematical models, the second-order-interaction model and the third-order-interaction model, to describe the dynamics of very sparse swarms and dense swarms, respectively. Based on these models, we have defined

a third mathematical model that allows us to investigate a continuous transition between the node-degree-based density of the second-order-interaction model and that of the third-order-interaction model. The third, intermediate model is obtained as a linear combination of the two models through the node-degree-based density parameter d, and is used to describe sparse swarms.

In the second-order-interaction model, negative feedback dominates the dynamics of the decision-making process, and noise-induced bistability can emerge only if the swarm is small; therefore, the system is not scalable. Systems that are modeled using the third-order-interaction model are bistable whenever the positive feedback generated by the majority rule dominates over the agent noise (i.e., noise introduced by spontaneous switching). These systems scale with swarm size and converge to a collective decision. However, the MFPT between the two stable states increases exponentially with the swarm size in these systems, which shows therefore a limited adaptivity to a dynamic environment (i.e., the system has difficulties in overturning a decision). By means of the intermediate model, we have investigated the transition from second-order interactions to third-order interactions with constant density-independent agent noise implemented by spontaneous switching. The change in swarm node-degree-based density results in a qualitative change of the decision dynamics from dominant negative feedback (unistable stationary distribution) to dominant positive feedback (bistable stationary distribution, cf. [43]). We validated our mathematical approach through extensive agent-based simulations, in which we considered aspects of the system such as spatial density and motion. The results show that the agent-based simulations match the predictions of the mathematical model.

Our starting point was the model of Biancalani et al. [4]. However, it is questionable whether Biancalani et al. [4] made a good choice in picking the Ohkubo system to model recruitment in ant foraging. Any noise-induced bistable system does not scale by definition because a critical swarm size exists. Such a foraging system would therefore not comply with the definition of swarm intelligence that requires scalability [5]. Any swarm system that relies on noise-induced bistability would hence be required to have a second mode of operation that governs super-critical swarm sizes. An example of how natural systems deal with challenges imposed by small swarm sizes is task switching during nest construction in

wasps [21, 13]. Small swarms have more frequently switching generalists to prevent slow-downs or deadlocks due to finite size effects (e.g., long waiting times for material transfers).

In this paper, we have focused on collective decision-making and in particular on the majority rule. We argue that the majority rule, with its minimal group size of three (node degree of two), is a prototypical example of which behavioral features influence the scalability of collective systems. Other examples of behavioral features that influence the system's scalability and that crucially depend on the swarm density are waiting times in object manipulation [20] or aggregation [35], as well as scaling of gradient values for localization in self-assembly [33]. Hence, we anticipate that our findings might generalize well.

We have explained the relevance of our findings to swarm intelligence in two exemplary interpretations. First, there can be a minimal critical swarm density in systems with swarm intelligence. For densities below that critical density the system fails (e.g., we would get an unistable stationary distribution in a collective decision-making system), although agents still approach each other and interact for very small densities $d \ll 0$. However, the modeled system is either too big or is characterized by a reaction rate coefficient r_1 that is too high to achieve noise-induced bistability. Second, any real collective system has a nonuniform distribution of agents in space. While it might be tempting to assume a uniform distribution when a particular average swarm density is given, the actual swarm distribution will be nonuniform. Consequently, the variance in the swarm density becomes relevant. If the swarm density variance is high, which is often the case in swarm systems (e.g., see [35, 15]), then there are areas of both high and low density. The fraction of the swarm N_h/N operating in an area of high density d_h is probably effective, but the fraction of the swarm N_l/N operating in an area of low density d_l is probably ineffective or even obstructive with respect to the swarm capacity of making a collective decision. Hence, whether a collective system is effective for a given swarm density and whether it scales to lower and higher densities depends on the nonuniform agent distribution. Similarly, the spatial distribution of agents determines which part of Fig. 13 represents the swarm performance (either the high density part $d \approx d_h$ or the low density part $d \approx d_l$). In addition, modeling techniques that represent only mean values for the limit $N \to \infty$ neglect

the variance and are consequently incapable of modeling these crucial finite-size effects. Furthermore, many collective systems are effective exactly because they succeed in generating the required network dynamics that creates desired node degree distributions (i.e., desired swarm densities) in a self-organizing process.

As a consequence, we argue that node degree distributions in collective systems are crucial for scalability investigations. Usually, collective systems need to be interpreted as dynamic networks, which are challenging to model [30, 17, 43]. Graphs generated by PPP have Poisson-distributed node degrees as discussed in Sec. 3.2. The Poisson distribution with the parameter λ has both mean and variance equal to λ. This could indicate a challenge for a dense system such as a swarm under the assumption that PPP represents a reasonable network model. For example, in a swarm where an average node degree of $\lambda = 11$ can be observed, the variance will also be $\lambda = 11$. Hence, there is a swarm fraction that should not be overlooked with node degrees down to even two and three. If those parts of the swarm that operate in low density areas are ineffective or even obstructive, then one might overestimate the scalability of the swarm.

The efficiency of a collective system has to be guaranteed for a minimal swarm density and for a minimal swarm size based on an assumed homogeneous distribution of agents. However, it is necessary to go beyond these requirements and efficiency also needs to be guaranteed when there is variance in the swarm density—a common feature of collective systems due to nonuniform agent distributions. These nonuniform distributions increase the importance of analyzing finite size effects that influence the system negatively. For example, in a collective decision-making system, agents from a very sparse region might permanently prevent convergence by getting in contact with a denser region often enough to disturb the system but also too infrequently to be recruited at large extent. The required analysis of finite size effects may be complex as also indicated by the situation shown in the bifurcation diagram in Fig. 13: a swarm effect that can be interpreted as a discrete jump from an ineffective state (unistable) for $d^* < -0.232$ to an effective state (bistable) for $d^* > -0.232$. Such a qualitative change in the behavior probably depends more on the swarm density than on the swarm size except for rather specific situations such as a required number of agents to build a bridge or

to push an object. Consequently, a more reasonable definition of scalability may be scalability over node-degree-based density.

Acknowledgments.

This work was partially supported by the European Union's Horizon 2020 research and innovation program under the FET grant '*flora robotica*', no. 640959.

Appendix A: Agent density in terms of area

For a given swarm size N and a given area A the swarm density is given by $\rho = N/A$. For simplicity we set the area to $A = 1$ [space unit]. We also require the concept of a critical swarm size N_c that corresponds to a critical swarm density $\rho_c = N_c/A = N_c$.

The node degree λ, as mentioned above, defines the group size $\lambda + 1$ of an agent. We compute the area A_s covered by an agent's sensor as $A_s = \pi u^2$ (for sensor range u), and we assume $A_s \ll A$. We get the expected node degree

$$\lambda = \rho A_s = N A_s. \tag{28}$$

Hence, the swarm density is defined in terms of swarm size N and node degree λ or group size $\lambda + 1$ for fixed sensor range u, where N or ρ can be varied. Note that the uniform distribution used for the agents approaches the imposed density ρ averaged over big areas but may vary considerably within small areas because the agents are not distributed with equidistant positions. Hence, the local node degrees vary as well.

Appendix B: Computation of MFPT of a Markov chain model

For a Markov chain model we can compute the MFPT from state i to state j [19, 18] as

$$m_{i,j} = p_{i,j} + \sum_{k \neq j} p_{i,k}(m_{k,j} + 1), \tag{29}$$

for the transition probability matrix P of the Markov chain with entries $p_{i,j}$. Our Markov chain is ergodic, thus the mean first passage time can be computed using the fundamental matrix F of the Markov chain which is defined as

$$F = (I - P + S)^{-1}, \tag{30}$$

where I is the identity matrix and $S = \lim_{t\to\infty} P^t$ is a matrix whose rows are equal to each other and given by the stationary distribution s. An entry $f_{i,j}$ of F gives the expected number of visits to transient state s_j if the system is started in transient state s_i. Here we can compute M with entries $m_{i,j}$ giving the MFPT from state i to state j using the fundamental matrix of the ergodic chain by

$$m_{i,j} = \frac{f_{j,j} - f_{i,j}}{s_j}. \tag{31}$$

References

1. Angluin, D., Aspnes, J., and Eisenstat, D. (2008). A simple population protocol for fast robust approximate majority. *Distributed Computing*, 21(2):87–102.
2. Arnold, L. (2003). *Random Dynamical Systems*. Springer, Berlin, Germany.
3. Beckers, R., Deneubourg, J.-L., Goss, S., and Pasteels, J. M. (1990). Collective decision making through food recruitment. *Insectes sociaux*, 37(3):258–267.
4. Biancalani, T., Dyson, L., and McKane, A. J. (2014). Noise-induced bistable states and their mean switching time in foraging colonies. *Physical Review Letters*, 112:038101.
5. Dorigo, M., Birattari, M., and Brambilla, M. (2014). Swarm robotics. *Scholarpedia*, 9(1):1463.
6. Dussutour, A., Beekman, M., Nicolis, S. C., and Meyer, B. (2009). Noise improves collective decision-making by ants in dynamic environments. *Proceedings of the Royal Society London B*, 276:4353–4361.
7. Dyson, L., Yates, C., Buhl, J., and McKane, A. (2015). Onset of collective motion in locusts is captured by a minimal model. *Physical Review E*, 92(5):052708.
8. Galam, S. (2000). Real space renormalization group and totalitarian paradox of majority rule voting. *Physica A: Statistical Mechanics and its Applications*, 285(1–2):66–76.

9. Gardiner, C. W. (1985). *Handbook of Stochastic Methods for Physics, Chemistry and the Natural Sciences*. Springer, Berlin, Germany.
10. Grüter, C., Schürch, R., Czaczkes, T., Taylor, K., Durance, T., Jones, S., and Ratnieks, F. (2012). Negative feedback enables fast and flexible collective decision-making in ants. *PloS ONE*, 7(9):e44501.
11. Gutiérrez, Á., Campo, A., Monasterio-Huelin, F., Magdalena, L., and Dorigo, M. (2010). Collective decision-making based on social odometry. *Neural Computing and Applications*, 19(6):807–823.
12. Halloy, J., Sempo, G., Caprari, G., Rivault, C., Asadpour, M., Tâche, F., Saïd, I., Durier, V., Canonge, S., Amé, J. M., Detrain, C., Correll, N., Martinoli, A., Mondada, F., Siegwart, R., and Deneubourg, J.-L. (2007). Social integration of robots into groups of cockroaches to control self-organized choices. *Science*, 318(5853):1155–1158.
13. Hamann, H., Karsai, I., and Schmickl, T. (2013). Time delay implies cost on task switching: A model to investigate the efficiency of task partitioning. *Bulletin of Mathematical Biology*, 75(7):1181–1206.
14. Hamann, H., Valentini, G., Khaluf, Y., and Dorigo, M. (2014). Derivation of a micro-macro link for collective decision-making systems: Uncover network features based on drift measurements. In Bartz-Beielstein, T., Branke, J., Filipič, B., and Smith, J., editors, *13th International Conference on Parallel Problem Solving from Nature (PPSN 2014)*, volume 8672 of *LNCS*, pages 181–190. Springer.
15. Hamann, H. and Wörn, H. (2008). A framework of space-time continuous models for algorithm design in swarm robotics. *Swarm Intelligence*, 2(2-4):209–239.
16. Houchmandzadeh, B. and Vallade, M. (2015). Exact results for a noise-induced bistable system. *Physical Review E*, 91(2):022115.
17. Huepe, C., Zschaler, G., Do, A.-L., and Gross, T. (2011). Adaptive-network models of swarm dynamics. *New Journal of Physics*, 13(7):073022.
18. Hunter, J. J. (2005). Stationary distributions and mean first passage times of perturbed markov chains. *Linear Algebra and its Applications*, 410:217–243.
19. Hunter, J. J. (2007). Simple procedures for finding mean first passage times in markov chains. *Asia-Pacific Journal of Operational Research*, 24(06):813–829.

20. Ijspeert, A. J., Martinoli, A., Billard, A., and Gambardella, L. M. (2001). Collaboration through the exploitation of local interactions in autonomous collective robotics: The stick pulling experiment. *Autonomous Robots*, 11:149–171.

21. Jeanne, R. L. (1986). The organization of work in *Polybia occidentalis*: Costs and benefits of specialization in a social wasp. *Behavioral Ecology and Sociobiology*, 19(5):333–341.

22. Khaluf, Y. and Dorigo, M. (2016). Modeling robot swarms using integrals of birth-death processes. *ACM Transactions on Autonomous and Adaptive Systems (TAAS)*, 11(2):8.

23. Khaluf, Y. and Hamann, H. (2016). On the definition of self-organizing systems: Relevance of positive/negative feedback and fluctuations. In *ANTS 2016*, volume 9882 of *LNCS*, page 298. Springer.

24. Lerman, K., Martinoli, A., and Galstyan, A. (2005). A review of probabilistic macroscopic models for swarm robotic systems. In Şahin, E. and Spears, W. M., editors, *Swarm Robotics - SAB 2004 International Workshop*, volume 3342 of *LNCS*, pages 143–152. Springer.

25. Mallon, E., Pratt, S., and Franks, N. (2001). Individual and collective decision-making during nest site selection by the ant *Leptothorax albipennis*. *Behavioral Ecology and Sociobiology*, 50(4):352–359.

26. Martinoli, A., Easton, K., and Agassounon, W. (2004). Modeling swarm robotic systems: A case study in collaborative distributed manipulation. *International Journal of Robotics Research*, 23(4):415–436.

27. Meyer, B., Beekman, M., and Dussutour, A. (2008). Noise-induced adaptive decision-making in ant-foraging. In *Simulation of Adaptive Behavior (SAB)*, number 5040 in LNCS, pages 415–425. Springer.

28. Montes de Oca, M., Ferrante, E., Scheidler, A., Pinciroli, C., Birattari, M., and Dorigo, M. (2011). Majority-rule opinion dynamics with differential latency: A mechanism for self-organized collective decision-making. *Swarm Intelligence*, 5(3–4):305–327.

29. Ohkubo, J., Shnerb, N., and Kessler, D. A. (2008). Transition phenomena induced by internal noise and quasi-absorbing state. *Journal of the Physical Society of Japan*, 77(4):044002.

30. Olfati-Saber, R., Fax, A., and Murray, R. M. (2007). Consensus and cooperation in networked multi-agent systems. *Proceedings of the IEEE*, 95(1):215–233.
31. Reina, A., Miletitch, R., Dorigo, M., and Trianni, V. (2015a). A quantitative micro–macro link for collective decisions: the shortest path discovery/selection example. *Swarm Intelligence*, 9(2-3):75–102.
32. Reina, A., Valentini, G., Fernández-Oto, C., Dorigo, M., and Trianni, V. (2015b). A design pattern for decentralised decision making. *PLoS ONE*, 10(10):e0140950.
33. Rubenstein, M., Cornejo, A., and Nagpal, R. (2014). Programmable self-assembly in a thousand-robot swarm. *Science*, 345(6198):795–799.
34. Saffre, F., Furey, R., Krafft, B., and Deneubourg, J.-L. (1999). Collective decision-making in social spiders: Dragline-mediated amplification process acts as a recruitment mechanism. *Journal of Theoretical Biology*, 198:507–517.
35. Schmickl, T. and Hamann, H. (2011). BEECLUST: A swarm algorithm derived from honeybees. In Xiao, Y., editor, *Bio-inspired Computing and Communication Networks*. CRC Press.
36. Seeley, T. D., Camazine, S., and Sneyd, J. (1991). Collective decision-making in honey bees: how colonies choose among nectar sources. *Behavioral Ecology and Sociobiology*, 28(4):277–290.
37. Seeley, T. D., Visscher, P., Schlegel, T., Hogan, P., Franks, N., and Marshall, J. (2012). Stop signals provide cross inhibition in collective decision-making by honeybee swarms. *Science*, 335(6064):108–111.
38. Streit, R. (2010). *Poisson Point Processes: Imaging, Tracking, and Sensing*. Springer, New York, USA.
39. Szopek, M., Schmickl, T., Thenius, R., Radspieler, G., and Crailsheim, K. (2013). Dynamics of collective decision making of honeybees in complex temperature fields. *PLoS ONE*, 8(10):e76250.
40. Togashi, Y. and Kaneko, K. (2001). Transitions induced by the discreteness of molecules in a small autocatalytic system. *Physical Review Letters*, 86:2459–2462.
41. Valentini, G., Ferrante, E., and Dorigo, M. (2017). The best-of-n problem in robot swarms: Formalization, state of the art, and novel perspectives. *Frontiers in Robotics and AI*, 4:9.

42. Valentini, G., Ferrante, E., Hamann, H., and Dorigo, M. (2015). Collective decision with 100 Kilobots: Speed versus accuracy in binary discrimination problems. *Autonomous Agents and Multi-Agent Systems*, 30(3):553–580.

43. Valentini, G. and Hamann, H. (2015). Time-variant feedback processes in collective decision-making systems: Influence and effect of dynamic neighborhood sizes. *Swarm Intelligence*, 9(2-3):153–176.

44. Valentini, G., Hamann, H., and Dorigo, M. (2014). Self-organized collective decision making: The weighted voter model. In Lomuscio, A., Scerri, P., Bazzan, A., and Huhns, M., editors, *Proceedings of the 13th International Conference on Autonomous Agents and Multiagent Systems*, AAMAS '14, pages 45–52. IFAAMAS.

45. Yates, C., Erban, R., Escudero, C., Couzin, I., Buhl, J., Kevrekidis, I., Maini, P., and Sumpter, D. (2009). Inherent noise can facilitate coherence in collective swarm motion. *PNAS*, 106(14):5464–5469.